DIRECTIONAL ANALYSIS OF DIGITIZED PLANAR SETS BY CONFIGURATION COUNTS

E.B.V. JENSEN,* *University of Aarhus*

M. KIDERLEN,** *University of Karlsruhe*

Abstract

The directional distribution of a random set Z can be used to quantify its anisotropy. A method for estimating this quantity from a digitization of Z in a sampling window, i.e. its pixel image, is presented. The image is analyzed locally by considering pixel squares of size $n \times n$. This allows to count the number of different types of $n \times n$ configurations in the pixel image. In the present paper, it is shown that it suffices to restrict attention to the so-called informative configurations. The number of informative configurations increases only polynomially in n. An algorithm to find these informative configurations is presented. Furthermore, estimators of the directional distribution based on counts of observed informative configurations are derived. The procedure is illustrated by a simulated example and an analysis of a microscopic image of steel.

Keywords: digitization; oriented rose of directions; length density; stationary random set; mean normal measure

1. Introduction

The rose of normal directions is commonly used for the detection and analysis of anisotropies in homogeneous planar structures, see Stoyan et al. [8]. For a structure consisting of fibres, the direct way to obtain the rose of normal directions is to measure the normal directions from a set of typical points on the fibres, selected with uniform probability. If the estimation procedure is supposed to be automized or if only digitized

* Postal address: Laboratory for Computional Stochastics and MaPhySto, Department of Mathematical Sciences, University of Aarhus, Ny Munkegade, DK–8000 Aarhus C, Denmark

** Postal address: Mathematical Institute II, University of Karlsruhe, D-76128 Karlsruhe, Germany

images are available, the rose is estimated by comparing neighbouring pixels in the digitized image (see below).

This procedure can also be applied to structures that consist of two or more phases, considering the phase boundaries. More specifically, if $Z \subset \mathbb{R}^2$ is the (sufficiently regular) phase of interest, the rose of normal directions of the boundary $\mathrm{bd}Z$ can be determined. It describes the distribution of the normal direction at a typical point of $\mathrm{bd}Z$. However, it is more natural to consider the distribution of the *outer unit normal vector* at a typical point of $\mathrm{bd}Z$, thus using the information that $\mathrm{bd}Z$ separates the two phases Z and its complement Z^C. The resulting distribution is called the *oriented rose of normal directions* or the *directional distribution of* Z. The usual procedure to estimate the rose of normal directions by comparing neighbouring pixels is not sufficient to estimate the oriented rose. In the present paper, we present a new method, where not only pairs of pixels but pixel squares of size 2×2 or larger are used to analyze the image. In Kiderlen & Jensen [4], the theoretical basis of the method has been developed and the information available in pixel squares of size 2×2 has been studied. In the present paper, the focus is on pixel squares of arbitrary size.

The idea of using pixel squares has been suggested by Ohser et al. [5] and Ohser & Mücklich [6] to estimate the length density and the density of the Euler characteristics of Z. If B and W are two non-overlapping sets that form an $n \times n$ pixel square, then the probability

$$p_{B,W}(t) := P(tB \subset Z, tW \subset Z^C) \tag{1.1}$$

(where t is a scaling factor) can efficiently be estimated by filtering the discretized image. (B stands for 'black' points belonging to the random set Z, W for 'white' points not hitting Z.) This is the reason, why we also restrict attention to such subsets B, W. The number of possible subsets (B, W) of the $n \times n$ pixel square increases exponentially in n. One of our main findings is that for inference on the directional distribution of Z it suffices to consider a subset T_n of informative configurations (B, W). The number of informative configurations increases only polynomially in n. Yet, the configurations in T_n lead to the same information on the directional distribution as *all* pairs of subsets of the $n \times n$ pixel square.

The paper is organized as follows: In the next section we define the mean normal

measure and the oriented rose of normal directions. Also, the traditional procedure to estimate the un-oriented rose by comparing neighbouring pixels is recalled in this section. In Section 3, we describe in more detail how to estimate the probabilities (1.1) from the discretization of a random set. In Section 4, inference about the directional distribution of Z based on observation of events of the type $tB \subset Z, tW \subset Z^C$ is discussed. An approximation to (1.1), valid for small t, is presented and discussed in Section 4.1. Furthermore, an algorithm for finding the set T_n of informative configurations is suggested and a simple procedure for calculating the probability of observing an informative configuration is given. In Section 4.2, estimators for the mean normal measure will be given explicitly for n =2 and 3. A simulated image and a microscopic image of steel will be analyzed in Section 5, illustrating the new approach. In Section 6, considerations concerning information are presented.

2. The mean normal measure and the oriented rose

In the following we will specify the notions and concepts used. Consider a random set $Z \subset \mathbb{R}^2$. We assume stationarity (i.e. homogeneity with respect to all translations). It is convenient to define the *mean normal measure* $\mathcal{L}$ *of* Z, the normalization of which is the oriented rose. $\mathcal{L}$, a measure on the unit circle S^1 of $\mathbb{R}^2$, has been introduced by Weil [9], [10]. Consider a subset B of S^1 and let $N_Z(B)$ be the part of the boundary of Z with *outer* unit normal in B, cf. Figure 1. Let $W \subset \mathbb{R}^2$ be a window with positive, finite area and let $L(N_Z(B) \cap W)$ be the length measure of the part of $N_Z(B)$ contained in W.

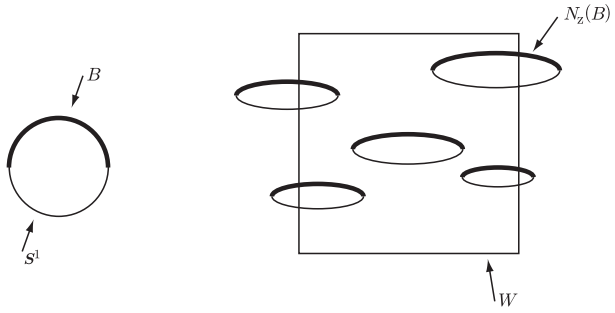

Figure 1: The set Z is a union of particles of elliptic shape. The set B of directions is the upper half of S^1 (left) while $N_Z(B)$ is the thickly drawn part of the boundary of Z (right).

If we normalize the expected value of $L(N_Z(B)\cap W)$ with respect to the area $\mathrm{A}(W)$ of W, we obtain the mean normal measure

$$\mathcal{L}(\cdot) = \frac{\mathbb{E}L\left(N_Z\left(\cdot\right)\cap W\right)}{\mathrm{A}(W)}.$$

The stationarity of Z ensures that this definition is independent of the window W.

The following observation is crucial for the construction of the estimators of $\mathcal{L}$ in Section 4.2: The boundary of a convex particle K (e.g. one of the ellipses in Figure 1) is clearly a closed curve. Mathematically, this can be expressed by saying that the boundary length measure $L(N_K(\cdot))$ of K has a centroid coinciding with the origin. The measure $\mathcal{L}$ inherits this property and hence we have

$$\int_{S^1} u\,\mathrm{d}\mathcal{L}(u) = 0. \tag{2.1}$$

(Recall that an integral on S^1 has the following simple interpretation. For $f : S^1 \to \mathbb{R}$ we have

$$\int_{S^1} f(u)\mathrm{d}\mathcal{L}(u) = \int_0^{2\pi} f(\cos\varphi, \sin\varphi)\,\mathrm{d}\bar{\mathcal{L}}(\varphi),$$

where $\bar{\mathcal{L}}$ is the mean normal measure represented as a measure on $[0, 2\pi)$. The centroid property (2.1) can be written as

$$\int_0^{2\pi} \cos\varphi\mathrm{d}\bar{\mathcal{L}}(\varphi) = \int_0^{2\pi} \sin\varphi\mathrm{d}\bar{\mathcal{L}}(\varphi) = 0.)$$

Note that the total mass of the mean normal measure is the length density

$$L_A = \mathcal{L}(S^1). \tag{2.2}$$

We will assume throughout the following that $0 < L_A < \infty$ holds. Then, the normalization $\mathcal{R}_{\mathrm{o}}(\cdot) = \mathcal{L}(\cdot)/L_A$ is the *oriented rose of normal directions*, the quantity, we are interested in. If we symmetrize $\mathcal{R}_{\mathrm{o}}$, we obtain the (un-oriented) rose of normal directions of $\mathrm{bd}Z$

$$\mathcal{R} = \frac{1}{2}\left(\mathcal{R}_{\mathrm{o}} + \mathcal{R}_{\mathrm{o}}^*\right),$$

as we do not distinguish between outer and inner normal directions. Here, $\mathcal{R}_{\mathrm{o}}^*$ is obtained from $\mathcal{R}_{\mathrm{o}}$ by replacing outer normals with inner normals. (Phrased more abstractly, the measure $\mathcal{R}_{\mathrm{o}}^*$ is the reflection of $\mathcal{R}_{\mathrm{o}}$ at the origin.)

A digitization (or discretization) of Z is the intersection of Z with a scaled lattice. For a fixed scaling factor $t > 0$, we consider $Z \cap t\mathbb{L}$, where

$$\mathbb{L} := \mathbb{Z}^2 = \{(i, j) \mid i, j \in \mathbb{Z}\}$$

is the usual lattice of points with integer coordinates. Other lattices, for example those with hexagonal cells, have been considered in the literature (e.g. [7]). Although the methods could be applied to these lattices as well, we restrict here to the usual lattice as it is the most important for applications. The *lattice square*

$$\mathbb{L}_n := \{(i, j) \mid i, j = 0, \ldots, n \Leftrightarrow 1\}$$

consists of n^2 points ($n > 1$). A line passing through at least two points of $\mathbb{L}_n$ will be called an *n–lattice line*.

To estimate the (un-oriented) rose of normal directions $\mathcal{R}$ from the discretized set $Z \cap t\mathbb{L}$, Serra [7] suggested to consider pairs of lattice points. See also Kärkkäinen et al. [2], [3], Ohser & Mücklich [6] and references therein. If b and w are two points of the un-scaled lattice, then the probability

$$p_{b,w}(t) := \mathbb{P}(tb \in Z, tw \notin Z) = \mathbb{P}(tb \in Z \cap t\mathbb{L}, tw \notin Z \cap t\mathbb{L}) \tag{2.3}$$

can be estimated from the discretized set $Z \cap t\mathbb{L}$. Indeed, due to the stationarity of Z, the relative number of translated point pairs $tb + x, tw + x \in t\mathbb{L}$ in the sampling window with $tb + x \in Z, tw + x \notin Z$ yields an estimator for $p_{b,w}(t)$. Under regularity conditions, we have

$$\lim_{t \to 0+} \frac{1}{t} p_{b,w}(t) = \frac{1}{2} \int_{S^1} |\langle b \Leftrightarrow w, v \rangle| \, \mathrm{d}\mathcal{L}(v). \tag{2.4}$$

((2.4) is proved for example in Kiderlen & Jensen [4], under the condition that Z locally is a finite union of convex sets with interior points. In what follows, Z will be assumed to fulfil this condition.) Here, $\langle b \Leftrightarrow w, v \rangle$ denotes the usual inner product of $b \Leftrightarrow w$ and v. Recall that for two vectors x and y in the plane

$$\langle x, y \rangle = \|x\| \cdot \|y\| \cdot \cos \sphericalangle(x, y),$$

where $\|x\|$ denotes the length of the vector x and $\sphericalangle(x, y)$ is the angle between the vectors x and y. Since $\|v\| = 1$ for $v \in S^1$, we thus have for small scaling factors t

$$\frac{p_{b,w}(t)}{\|tb \Leftrightarrow tw\|} \doteq \frac{L_A}{2} \int_{S^1} |\cos \sphericalangle(b \Leftrightarrow w, v)| \mathrm{d}\mathcal{R}_{\circ}(v). \tag{2.5}$$

Formula (2.5) connects observations based on comparison of pairs of points from the discretized set to an integral transform (the so called *cosine transform*) of $\mathcal{R}_o$.

As the integrand in (2.5) remains unchanged if v is replaced with $\Leftrightarrow v$, $\mathcal{R}_o$ and $\mathcal{R}_o^*$ have the same cosine transform. Hence, the oriented rose of normal directions $\mathcal{R}_o$ cannot be determined using (2.5). This shows that the information from *pairs* of lattice points is not sufficient to determine the oriented rose. Theoretically, the right hand side of (2.5) determines the un-oriented rose $\mathcal{R}$ uniquely, if the normalization of $b \Leftrightarrow w$ runs through all of S^1 (see e.g. page 379 in GARDNER [1]). Note, however, that using discretized images, the number of point pairs and hence the number of natural orientations in (2.4) is always finite. Therefore only approximations of the un-oriented rose can be obtained this way.

3. Configuration counts by filtering

In this section, we will briefly describe how counts of $n \times n$ configurations can be performed by the simple linear filtering procedure, described e.g. in OHSER ET AL. [5]. An $n \times n$ configuration (with scaling factor t) is a subset tB of the scaled lattice square $t\mathbb{L}_n$. Usually, we will illustrate the configuration by $n \times n$ points such that elements from tB are shown as 'black' points and elements from $tW = t\mathbb{L}_n \backslash tB$ are shown as 'white' points. As an example, for $n = 2$ the notation $\left[\begin{smallmatrix} \circ & \bullet \\ \bullet & \bullet \end{smallmatrix}\right]_t$ stands for the pair (tB, tW) with $B = \{(0,0),(1,0),(1,1)\}$ and $W = \{(0,1)\}$. The index t indicates the scaling.

The set of $n \times n$ configurations is in one-to-one correspondence with the integers $0, 1, \ldots, 2^{n^2} \Leftrightarrow 1$. One way of establishing this correspondence is as follows. Let us represent a configuration given by $tB \subseteq t\mathbb{L}_n$ as an $n \times n$ matrix

$$\{z_{hl} | h, l = 0, \ldots, n \Leftrightarrow 1\},$$

where $z_{hl} = 1$, if $(h,l) \in B$ and $z_{hl} = 0$, otherwise. Furthermore, let F_n be the $n \times n$ matrix with elements

$$f_{hl} = 2^{h+nl},$$

$h, l = 0, \ldots, n \Leftrightarrow 1$. Then, we can associate to the configuration the number

$$g_B = \sum_{h=0}^{n-1} \sum_{l=0}^{n-1} z_{hl} f_{hl}.$$

For instance, for the configuration $\begin{bmatrix} \circ & \bullet \\ \bullet & \bullet \end{bmatrix}_t$ with $B = \{(0,0), (1,0), (1,1)\}$ we get

$$g_B = 1 \cdot 2^0 + 1 \cdot 2^1 + 0 \cdot 2^2 + 1 \cdot 2^3 = 11.$$

Let us now consider a binary image of size $k \times m$

$$\mathcal{Z} = \{z_{ij} | i = 0, \ldots, k \Leftrightarrow 1, j = 0, \ldots, m \Leftrightarrow 1\},$$

where $k, m \geq n$ and $z_{ij} = 1$, if $(it, jt) \in Z$, and $z_{ij} = 0$, otherwise. For each $tB \subseteq t\mathbb{L}_n$, we want to count the number of configurations of type B in the image, i.e. the number of translated pairs $tB + x, tW + x$ contained in $\{0, \ldots, k \Leftrightarrow 1\} \times \{0, \ldots, m \Leftrightarrow 1\}$ such that $tB + x \subseteq Z$ and $tW + x \subseteq Z^C$. This information is available in the grey-tone image

$$\mathcal{G} = \{g_{ij} | i = 0, \ldots, k \Leftrightarrow n, j = 0, \ldots, m \Leftrightarrow n\}$$

obtained by linear filtering of $\mathcal{Z}$ with F_n. Here,

$$g_{ij} = \sum_{h=0}^{n-1} \sum_{l=0}^{n-1} z_{i+h, j+l} f_{hl}.$$

The number of configurations of type B is equal to the number of pixels in $\mathcal{G}$ with value g_B. This number can be calculated very efficiently using binary operations, avoiding the explicit calculation of $\mathcal{G}$, cf. Ohser et al. [5]. The approach is illustrated in Figure 2.

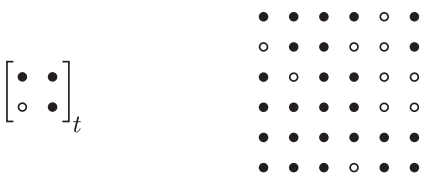

Figure 2: Illustration of configuration counts. Here $n = 2$, $k = m = 6$, $B = \{(1,0), (0,1), (1,1)\}$, $g_B = 14$ and the number of configurations of type B is 3.

4. The mean normal measure and $n \times n$ configurations

4.1. Informative configurations

In analogy to the classical procedure, we now present a formula connecting the information obtained from the discretized random set and properties of the mean normal measure. Let $B \subseteq \mathbb{L}_n$, $n > 1$, and $W = \mathbb{L}_n \backslash B$ such that B and W are disjoint and together form $\mathbb{L}_n$. Generalizing (2.4), Theorem 4 in KIDERLEN & JENSEN [4] states that

$$\lim_{t \to 0+} \frac{1}{t} \mathbb{P}(tB \subset Z,\ tW \subset Z^C) = \int_{S^1} h_{(B,W)}(\Leftrightarrow v) \mathrm{d}\mathcal{L}(v), \tag{4.1}$$

where

$$h_{(B,W)}(v) = \left[\min_{b \in B} \langle b, v \rangle \Leftrightarrow \max_{w \in W} \langle w, v \rangle \right]^+, \quad v \in S^1. \tag{4.2}$$

(Here $f^+ := \max\{f, 0\}$ denotes the positive part of a function f.) The function $h_{(B,W)}$ has the following intuitive interpretation: Let $S(v)$ be the (possibly empty) union of all lines orthogonal to v, separating the sets W and B, in such a way that W lies in the negative half plane with respect to v. (For a precise definition of separation, cf. the first paragraph of Appendix A.) Then $h_{(B,W)}(v)$ is equal to the width of the strip $S(v)$, cf. Figure 3.

This interpretation is intuitive and shows that for small t, the boundary of Z can be thought of as a line g with outer unit normal v: The probability that a $n \times n$-square 'randomly thrown on g' allows the observation of the configuration (B, W) is proportional to the probability that g lies in $S(v)$, which in turn is proportional to the width of $S(v)$.

Definition (4.2) shows that $h_{(B,W)}$ is invariant under simultaneous translations of B and W. Moreover,

$$h_{(B,W)}(\Leftrightarrow v) = h_{(W,B)}(v)$$

and

$$h_{(\vartheta B, \vartheta W)}(\vartheta v) = h_{(B,W)}(v)$$

for any $v \in S^1$ and any rotation ϑ fixing the origin. Note that if $\mathcal{L}$ is symmetric, the integral in (4.1) remains the same if B and W are interchanged.

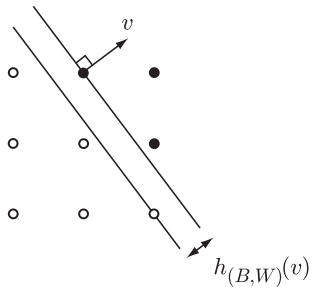

FIGURE 3: Illustration of the function $h_{(B,W)}$. For details, see text.

Several $n \times n$ configurations (B, W) can lead to the same function $h_{(B,W)}$. As an important example, consider the pair (B, W) and define *the twin pair* $(B, W)^*$ *of* (B, W) by $(B, W)^* = (B', W')$ with

$$B' := \rho_n(W), \qquad W' := \rho_n(B).$$

Here ρ_n denotes the reflection of a set at the midpoint $((n \Leftrightarrow 1)/2, (n \Leftrightarrow 1)/2)$ of $\mathbb{L}_n$. Thus, (B', W') is obtained by a reflection and a subsequent interchange, an operation, we will call *reflection-switch* in the following, cf. Figure 4. From the definition of $h_{(B,W)}$, it follows that

$$h_{(B,W)^*} = h_{(B,W)}.$$

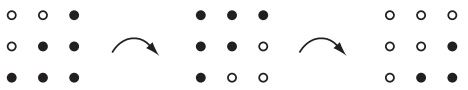

FIGURE 4: Consecutive reflection and switch of a configuration leading to its twin.

It is clear that the number of possible choices of (B, W) (with $\emptyset \neq B$, $\emptyset \neq W$, $B \cup W = \mathbb{L}_n$, $B \cap W = \emptyset$) is increasing exponentially in n: there are $2^{n^2} \Leftrightarrow 2$ such choices. But for most choices of (B, W), the function $h_{(B,W)}$ is identically zero, meaning that the probability of observing such a configuration goes to zero, as $t \to 0+$. A configuration (B, W) with a non-identically zero $h_{(B,W)}$ is called an *informative configuration*. From the geometric interpretation of $h_{(B,W)}$, it follows that (B, W) is informative if and only

if there is an $n\Leftrightarrow$lattice line separating B and W and not hitting both of them. (Here, Lemma 1 in the Appendix has been used.) For a given $n > 1$, the algorithm below determines the set T_n of informative $n \times n$ configurations.

Algorithm 1

0. *Set* $T_n := \emptyset$.
1. *Choose an n-lattice line* g. Decompose $\mathbb{L}_n$ in $g \cap \mathbb{L}_n$, H^+ and H^- where H^+ and H^- are the remaining lattice points on each side of g.
   1.1. Put $B = g \cup H^+$ and $W = H^-$. If W is not empty, then include (B, W) and its twin $(B, W)^*$ in T_n.
   1.2. Put $B = g \cup H^-$ and $W = H^+$. If W is not empty, then include (B, W) and its twin $(B, W)^*$ in T_n.
2. *Repeat 1. until all n-lattice lines have been considered.*
3. T_n *is the output.*

Note that the number of informative configurations is at most of order n^4.

It is important to have a simple way to determine the h function for a particular informative configuration. The theorem below gives such a simple description. The proof of this result can be found in Appendix A.

Theorem 1. *Let* $(B, W) \in T_n$ *be an informative configuration. Then, there exist vectors* $a, b \in \mathbb{R}^2$ *such that*

$$h_{(B,W)}(\Leftrightarrow v) = \min\{\langle a, v\rangle^+, \langle b, v\rangle^+\} \tag{4.3}$$

for all $v \in S^1$.

The construction of a and b for a given informative configuration (B, W) will be explained in the Appendix. For $n = 2$ and 3, the values of a and b are part of Table 1 and 2 below. A main step in the construction of a and b is to find a *reduced* configuration (B', W') such that $B' \subset B$, $W' \subset W$, $|B'| \leq 2$, $|W'| \leq 2$ and such that any line separating B' and W' separates also B and W. See also Figure 5.

FIGURE 5: An example of an informative 3×3 configuration (left) and its associated reduced configuration (right) where the dots indicate that the corresponding pixel may be black or white.

In the following table we list the output of Algorithm 1 for $n = 2$ together with the values for a and b. If the column for the twin pair contains '(s)', then the pair (B, W) under consideration is a self-twin, i.e.

$$(B, W)^* = (B, W).$$

There are 8 groups of configurations in T_n for $n = 2$. They are ordered according to increasing angle of $a + b$ with the $x \Leftrightarrow$axis.

No.	config.	twin	a	b
1	$\begin{bmatrix} \bullet & \circ \\ \bullet & \circ \end{bmatrix}_t$	(s)	$\begin{pmatrix} 1 \\ 1 \end{pmatrix}$	$\begin{pmatrix} 1 \\ -1 \end{pmatrix}$
2	$\begin{bmatrix} \bullet & \circ \\ \bullet & \bullet \end{bmatrix}_t$	$\begin{bmatrix} \circ & \circ \\ \bullet & \circ \end{bmatrix}_t$	$\begin{pmatrix} 0 \\ 1 \end{pmatrix}$	$\begin{pmatrix} 1 \\ 0 \end{pmatrix}$
3	$\begin{bmatrix} \circ & \circ \\ \bullet & \bullet \end{bmatrix}_t$	(s)	$\begin{pmatrix} -1 \\ 1 \end{pmatrix}$	$\begin{pmatrix} 1 \\ 1 \end{pmatrix}$
4	$\begin{bmatrix} \circ & \bullet \\ \bullet & \bullet \end{bmatrix}_t$	$\begin{bmatrix} \circ & \circ \\ \circ & \bullet \end{bmatrix}_t$	$\begin{pmatrix} 0 \\ 1 \end{pmatrix}$	$\begin{pmatrix} -1 \\ 0 \end{pmatrix}$
5	$\begin{bmatrix} \circ & \bullet \\ \circ & \bullet \end{bmatrix}_t$	(s)	$\begin{pmatrix} -1 \\ 1 \end{pmatrix}$	$\begin{pmatrix} -1 \\ -1 \end{pmatrix}$
6	$\begin{bmatrix} \bullet & \bullet \\ \circ & \bullet \end{bmatrix}_t$	$\begin{bmatrix} \circ & \bullet \\ \circ & \circ \end{bmatrix}_t$	$\begin{pmatrix} -1 \\ 0 \end{pmatrix}$	$\begin{pmatrix} 0 \\ -1 \end{pmatrix}$
7	$\begin{bmatrix} \bullet & \bullet \\ \circ & \circ \end{bmatrix}_t$	(s)	$\begin{pmatrix} -1 \\ -1 \end{pmatrix}$	$\begin{pmatrix} 1 \\ -1 \end{pmatrix}$
8	$\begin{bmatrix} \bullet & \bullet \\ \bullet & \circ \end{bmatrix}_t$	$\begin{bmatrix} \bullet & \circ \\ \circ & \circ \end{bmatrix}_t$	$\begin{pmatrix} 1 \\ 0 \end{pmatrix}$	$\begin{pmatrix} 0 \\ -1 \end{pmatrix}$

Table 1: The 8 groups of configurations in T_n for n=2.

For $n = 3$, we obtain the following table, where configurations with the same values of a and b are grouped. Each group consists of at most two configurations

and their twins. The first 16 groups are ordered as follows. For configuration No. i with corresponding a_i and b_i according to Table 2, let v_i be the unit vector for which the function

$$h_{a_i,b_i}(v) = \min\{\langle a_i, v\rangle^+, \langle b_i, v\rangle^+\}. \tag{4.4}$$

attains its maximum. Hence, v_i is the 'most probable' outer unit vector of Z given configuration No. i. Explicitly, v_i is the normalization of $\alpha_i a_i + \beta_i b_i$ with

$$\alpha_i := \|b_i\|^2 \Leftrightarrow\langle a_i, b_i\rangle, \qquad \beta_i := \|a_i\|^2 \Leftrightarrow\langle a_i, b_i\rangle.$$

(It turns out that the set of the 16 directions $\{v_1, \ldots, v_{16}\}$ is also the set of all directions of n-grid lines for $n = 3$.) The configurations No. $1, \ldots, 16$ are now ordered according to increasing angles of v_i with respect to the x-axis. The last 4 groups are related to the previous groups in the following way. Let

$$I_i = \int_{S^1} h_{a_i,b_i}(v)\mathrm{d}\mathcal{L}(v), \quad i = 1, \ldots, 20.$$

Then, $I_i, i = 17, 18, 19, 20$, can be expressed in terms of the other integrals, since

$$I_{i+16} = I_{4i-2} + I_{4i-1} + I_{4i}, \quad i = 1, 2, 3, 4. \tag{4.5}$$

The result (4.5) is most easily shown by direct calculation.

No.	config.	twin	config.	twin	a	b
1	$\begin{bmatrix}\bullet&\circ&\circ\\ \bullet&\circ&\circ\\ \bullet&\circ&\circ\end{bmatrix}_t$	$\begin{bmatrix}\bullet&\bullet&\circ\\ \bullet&\bullet&\circ\\ \bullet&\bullet&\circ\end{bmatrix}_t$	-	-	$\begin{pmatrix}1\\2\end{pmatrix}$	$\begin{pmatrix}1\\-2\end{pmatrix}$
2	$\begin{bmatrix}\bullet&\circ&\circ\\ \bullet&\circ&\circ\\ \bullet&\bullet&\circ\end{bmatrix}_t$	$\begin{bmatrix}\bullet&\circ&\circ\\ \bullet&\bullet&\circ\\ \bullet&\bullet&\circ\end{bmatrix}_t$	$\begin{bmatrix}\bullet&\bullet&\circ\\ \bullet&\bullet&\circ\\ \bullet&\bullet&\bullet\end{bmatrix}_t$	$\begin{bmatrix}\circ&\circ&\circ\\ \bullet&\circ&\circ\\ \bullet&\circ&\circ\end{bmatrix}_t$	$\begin{pmatrix}0\\1\end{pmatrix}$	$\begin{pmatrix}1\\-1\end{pmatrix}$
3	$\begin{bmatrix}\circ&\circ&\circ\\ \bullet&\circ&\circ\\ \bullet&\bullet&\circ\end{bmatrix}_t$	$\begin{bmatrix}\bullet&\circ&\circ\\ \bullet&\bullet&\circ\\ \bullet&\bullet&\bullet\end{bmatrix}_t$	-	-	$\begin{pmatrix}-1\\2\end{pmatrix}$	$\begin{pmatrix}2\\-1\end{pmatrix}$
4	$\begin{bmatrix}\bullet&\circ&\circ\\ \bullet&\bullet&\bullet\\ \bullet&\bullet&\bullet\end{bmatrix}_t$	$\begin{bmatrix}\circ&\circ&\circ\\ \circ&\circ&\circ\\ \bullet&\bullet&\circ\end{bmatrix}_t$	$\begin{bmatrix}\circ&\circ&\circ\\ \bullet&\circ&\circ\\ \bullet&\bullet&\bullet\end{bmatrix}_t$	$\begin{bmatrix}\circ&\circ&\circ\\ \bullet&\bullet&\circ\\ \bullet&\bullet&\bullet\end{bmatrix}_t$	$\begin{pmatrix}-1\\1\end{pmatrix}$	$\begin{pmatrix}1\\0\end{pmatrix}$
5	$\begin{bmatrix}\circ&\circ&\circ\\ \bullet&\bullet&\bullet\\ \bullet&\bullet&\bullet\end{bmatrix}_t$	$\begin{bmatrix}\circ&\circ&\circ\\ \circ&\circ&\circ\\ \bullet&\bullet&\bullet\end{bmatrix}_t$	-	-	$\begin{pmatrix}-2\\1\end{pmatrix}$	$\begin{pmatrix}2\\1\end{pmatrix}$
6	$\begin{bmatrix}\circ&\circ&\bullet\\ \bullet&\bullet&\bullet\\ \bullet&\bullet&\bullet\end{bmatrix}_t$	$\begin{bmatrix}\circ&\circ&\circ\\ \circ&\circ&\circ\\ \circ&\bullet&\bullet\end{bmatrix}_t$	$\begin{bmatrix}\circ&\circ&\circ\\ \circ&\circ&\bullet\\ \bullet&\bullet&\bullet\end{bmatrix}_t$	$\begin{bmatrix}\circ&\circ&\circ\\ \circ&\bullet&\bullet\\ \bullet&\bullet&\bullet\end{bmatrix}_t$	$\begin{pmatrix}1\\1\end{pmatrix}$	$\begin{pmatrix}-1\\0\end{pmatrix}$
7	$\begin{bmatrix}\circ&\circ&\bullet\\ \circ&\bullet&\bullet\\ \bullet&\bullet&\bullet\end{bmatrix}_t$	$\begin{bmatrix}\circ&\circ&\circ\\ \circ&\circ&\bullet\\ \circ&\bullet&\bullet\end{bmatrix}_t$	-	-	$\begin{pmatrix}1\\2\end{pmatrix}$	$\begin{pmatrix}-2\\-1\end{pmatrix}$
8	$\begin{bmatrix}\circ&\bullet&\bullet\\ \circ&\bullet&\bullet\\ \bullet&\bullet&\bullet\end{bmatrix}_t$	$\begin{bmatrix}\circ&\circ&\circ\\ \circ&\circ&\bullet\\ \circ&\circ&\bullet\end{bmatrix}_t$	$\begin{bmatrix}\circ&\circ&\bullet\\ \circ&\circ&\bullet\\ \circ&\bullet&\bullet\end{bmatrix}_t$	$\begin{bmatrix}\circ&\circ&\bullet\\ \circ&\bullet&\bullet\\ \circ&\bullet&\bullet\end{bmatrix}_t$	$\begin{pmatrix}0\\1\end{pmatrix}$	$\begin{pmatrix}-1\\-1\end{pmatrix}$
9	$\begin{bmatrix}\circ&\bullet&\bullet\\ \circ&\bullet&\bullet\\ \circ&\bullet&\bullet\end{bmatrix}_t$	$\begin{bmatrix}\circ&\circ&\bullet\\ \circ&\circ&\bullet\\ \circ&\circ&\bullet\end{bmatrix}_t$	-	-	$\begin{pmatrix}-1\\2\end{pmatrix}$	$\begin{pmatrix}-1\\-2\end{pmatrix}$
10	$\begin{bmatrix}\bullet&\bullet&\bullet\\ \circ&\bullet&\bullet\\ \circ&\bullet&\bullet\end{bmatrix}_t$	$\begin{bmatrix}\circ&\circ&\bullet\\ \circ&\circ&\bullet\\ \circ&\circ&\circ\end{bmatrix}_t$	$\begin{bmatrix}\circ&\circ&\bullet\\ \circ&\circ&\bullet\\ \circ&\circ&\bullet\end{bmatrix}_t$	$\begin{bmatrix}\circ&\bullet&\bullet\\ \circ&\bullet&\bullet\\ \circ&\circ&\bullet\end{bmatrix}_t$	$\begin{pmatrix}-1\\1\end{pmatrix}$	$\begin{pmatrix}0\\-1\end{pmatrix}$
11	$\begin{bmatrix}\circ&\bullet&\bullet\\ \circ&\circ&\bullet\\ \circ&\circ&\circ\end{bmatrix}_t$	$\begin{bmatrix}\bullet&\bullet&\bullet\\ \circ&\bullet&\bullet\\ \circ&\circ&\bullet\end{bmatrix}_t$	-	-	$\begin{pmatrix}-2\\1\end{pmatrix}$	$\begin{pmatrix}1\\-2\end{pmatrix}$
12	$\begin{bmatrix}\bullet&\bullet&\bullet\\ \circ&\circ&\bullet\\ \circ&\circ&\circ\end{bmatrix}_t$	$\begin{bmatrix}\bullet&\bullet&\bullet\\ \circ&\bullet&\bullet\\ \circ&\circ&\circ\end{bmatrix}_t$	$\begin{bmatrix}\bullet&\bullet&\bullet\\ \bullet&\bullet&\bullet\\ \circ&\circ&\bullet\end{bmatrix}_t$	$\begin{bmatrix}\circ&\bullet&\bullet\\ \circ&\circ&\circ\\ \circ&\circ&\circ\end{bmatrix}_t$	$\begin{pmatrix}-1\\0\end{pmatrix}$	$\begin{pmatrix}1\\-1\end{pmatrix}$
13	$\begin{bmatrix}\bullet&\bullet&\bullet\\ \circ&\circ&\circ\\ \circ&\circ&\circ\end{bmatrix}_t$	$\begin{bmatrix}\bullet&\bullet&\bullet\\ \bullet&\bullet&\bullet\\ \circ&\circ&\circ\end{bmatrix}_t$	-	-	$\begin{pmatrix}-2\\-1\end{pmatrix}$	$\begin{pmatrix}2\\-1\end{pmatrix}$
14	$\begin{bmatrix}\bullet&\bullet&\bullet\\ \bullet&\circ&\circ\\ \circ&\circ&\circ\end{bmatrix}_t$	$\begin{bmatrix}\bullet&\bullet&\bullet\\ \bullet&\bullet&\circ\\ \circ&\circ&\circ\end{bmatrix}_t$	$\begin{bmatrix}\bullet&\bullet&\bullet\\ \bullet&\bullet&\bullet\\ \bullet&\circ&\circ\end{bmatrix}_t$	$\begin{bmatrix}\bullet&\bullet&\circ\\ \circ&\circ&\circ\\ \circ&\circ&\circ\end{bmatrix}_t$	$\begin{pmatrix}1\\0\end{pmatrix}$	$\begin{pmatrix}-1\\-1\end{pmatrix}$
15	$\begin{bmatrix}\bullet&\bullet&\circ\\ \bullet&\circ&\circ\\ \circ&\circ&\circ\end{bmatrix}_t$	$\begin{bmatrix}\bullet&\bullet&\bullet\\ \bullet&\bullet&\circ\\ \bullet&\circ&\circ\end{bmatrix}_t$	-	-	$\begin{pmatrix}2\\1\end{pmatrix}$	$\begin{pmatrix}-1\\-2\end{pmatrix}$
16	$\begin{bmatrix}\bullet&\bullet&\circ\\ \bullet&\circ&\circ\\ \bullet&\circ&\circ\end{bmatrix}_t$	$\begin{bmatrix}\bullet&\bullet&\circ\\ \bullet&\bullet&\circ\\ \bullet&\circ&\circ\end{bmatrix}_t$	$\begin{bmatrix}\bullet&\bullet&\bullet\\ \bullet&\bullet&\circ\\ \bullet&\bullet&\circ\end{bmatrix}_t$	$\begin{bmatrix}\bullet&\circ&\circ\\ \bullet&\circ&\circ\\ \circ&\circ&\circ\end{bmatrix}_t$	$\begin{pmatrix}1\\1\end{pmatrix}$	$\begin{pmatrix}0\\-1\end{pmatrix}$
17	$\begin{bmatrix}\bullet&\bullet&\circ\\ \bullet&\bullet&\bullet\\ \bullet&\bullet&\bullet\end{bmatrix}_t$	$\begin{bmatrix}\circ&\circ&\circ\\ \circ&\circ&\circ\\ \bullet&\circ&\circ\end{bmatrix}_t$	-	-	$\begin{pmatrix}0\\1\end{pmatrix}$	$\begin{pmatrix}1\\0\end{pmatrix}$
18	$\begin{bmatrix}\circ&\bullet&\bullet\\ \bullet&\bullet&\bullet\\ \bullet&\bullet&\bullet\end{bmatrix}_t$	$\begin{bmatrix}\circ&\circ&\circ\\ \circ&\circ&\circ\\ \circ&\circ&\bullet\end{bmatrix}_t$	-	-	$\begin{pmatrix}0\\1\end{pmatrix}$	$\begin{pmatrix}-1\\0\end{pmatrix}$
19	$\begin{bmatrix}\bullet&\bullet&\bullet\\ \bullet&\bullet&\bullet\\ \circ&\bullet&\bullet\end{bmatrix}_t$	$\begin{bmatrix}\circ&\circ&\bullet\\ \circ&\circ&\circ\\ \circ&\circ&\circ\end{bmatrix}_t$	-	-	$\begin{pmatrix}-1\\0\end{pmatrix}$	$\begin{pmatrix}0\\-1\end{pmatrix}$
20	$\begin{bmatrix}\bullet&\bullet&\bullet\\ \bullet&\bullet&\bullet\\ \bullet&\bullet&\circ\end{bmatrix}_t$	$\begin{bmatrix}\bullet&\circ&\circ\\ \circ&\circ&\circ\\ \circ&\circ&\circ\end{bmatrix}_t$	-	-	$\begin{pmatrix}1\\0\end{pmatrix}$	$\begin{pmatrix}0\\-1\end{pmatrix}$

Table 2: The 20 groups of pairs in T_n for n=3.

4.2. Estimation of the mean normal measure

In this section, we will discuss how to estimate the mean normal measure from observations of the different types of $n \times n$ configurations.

Let us group the set of configurations into types such that configurations of the same type have the same h function. Let k_n be the number of types. For instance, $k_2 = 8$ and $k_3 = 20$, cf. Table 1 and 2. Let a_i and b_i be the vectors associated with the ith type of informative configuration and m_i the number of configurations of type i, $i = 1, \ldots, k_n$. The non-informative configurations will be combined in type 0. Recall that the non-informative configurations consist of (B, W) for which either $B = \emptyset$ or $W = \emptyset$ or there is no $n\Leftrightarrow$lattice line separating B and W and not hitting both of them.

Let the mean normal measure $\mathcal{L}$ be parametrized by $\theta \in \Theta$, where Θ is a subset of $\mathbb{R}^d$, say. Let $\mathcal{L}_\theta$ be the notation used for the mean normal measure with parameter θ and let

$$I_i(\theta) = \int_{S^1} h_{a_i,b_i}(v)\,\mathrm{d}\mathcal{L}_\theta(v), \quad i = 1, \ldots, k_n,$$

be the corresponding parametrized integrals where h_{a_i,b_i} is given in (4.4). Then, according to (4.1) and Theorem 1, the probability of observing a type i configuration is for small t, approximately,

$$p_i(\theta) = t m_i I_i(\theta), \quad i = 1, \ldots, k_n.$$

Clearly, the probability of observing a non-informative $n \times n$ configuration is then for small t, approximately,

$$p_0(\theta) = 1 \Leftrightarrow \sum_{i=1}^{k_n} p_i(\theta).$$

Now, let us suppose that we have observed n_i configurations of type i, $i = 0, 1, \ldots, k_n$. As suggested in Kiderlen & Jensen [4], we will use as estimate of θ a value $\hat{\theta} \in \Theta$, at which

$$\ell(\theta) = \sum_{i=0}^{k_n} n_i \ln p_i(\theta) = n_0 \ln(1 \Leftrightarrow \sum_{i=1}^{k_n} t m_i I_i(\theta)) + \sum_{i=1}^{k_n} n_i \ln(t m_i I_i(\theta)) \qquad (4.6)$$

is maximal (if such a value exists). The use of ℓ is motivated by statistical arguments. In particular, ℓ is closely related to the divergence of the observed frequencies from the corresponding probabilities $p_i(\theta), i = 0, \ldots, k_n$.

Let us discuss in more detail how the estimation can be done in the case where $\mathcal{L}$ is a discrete measure. Assume that it is concentrated on d directions $v_1, \ldots, v_d$ and that $\mathcal{L} = \mathcal{L}_\theta$ is parametrized by $\theta = (\theta_1, \ldots, \theta_d)$, where θ_i is the mass at the ith direction v_i, $i = 1, \ldots, d$. Because of (2.1), the parameters must satisfy

$$\sum_{i=1}^{d} \theta_i \cos\varphi_i = 0, \quad \sum_{i=1}^{d} \theta_i \sin\varphi_i = 0. \tag{4.7}$$

Under the discrete model, the integrals $I_i(\theta)$ are linear functions of θ. It can then be shown by straightforward methods that the function ℓ in (4.6) is a concave function. The problem of finding the maximum of ℓ is thereby a concave optimization problem with linear constraints and can be solved by using standard software such as GAMS.

Let us suppose that $n = 2$ such that 2×2 configurations are observed. Let $d = 8$. For the directions $v_1, \ldots, v_8$ we choose the sides and diagonals of the 2×2 lattice square, where $v_1, \ldots, v_8$ are ordered according to increasing angles with respect to the x-axis, starting with $v_1 = (1, 0)$. Then

$$I_i(\theta) = \alpha_i \theta_i, \quad i = 1, \ldots, 8, \tag{4.8}$$

where

$$\alpha_i = \max_{v \in S^1} h_{a_i, b_i}(v) = h_{a_i, b_i}(v_i), \qquad i = 1, \ldots, 8,$$

and (a_i, b_i) is given in Table 1. For $n = 2$, the problem is thereby to maximize (4.6), where $I_i(\theta)$ is given in (4.8), subject to the linear side conditions in (4.7) and

$$\theta_i \geq 0, i = 1, \ldots, 8, \quad \sum_{i=1}^{8} t m_i I_i(\theta) \leq 1.$$

Here, $m_i = 1$ for i odd and $m_i = 2$ for i even.

For $n = 3$, we again assume a discrete model supported by the lattice directions, i.e. by the 16 possible directions of 3-grid lines $v_1, \ldots, v_{16}$. Again, we order these according to increasing angle starting with $v_1 = (1, 0)$. Then

$$I_i(\theta) = \begin{cases} \alpha_i \theta_i & i = 1, \ldots, 16 \\ \sum_{j=0}^{2} \alpha_{4(i-16)-j} \theta_{4(i-16)-j} & i = 17, 18, 19, 20, \end{cases} \tag{4.9}$$

where

$$\alpha_i = \max_{v \in S^1} h_{a_i, b_i}(v) = h_{a_i, b_i}(v_i), \qquad i = 1, \ldots, 16.$$

For $n = 3$, the problem is thereby to maximize (4.6), with $I_i(\theta)$ given in (4.9), subject to the linear side conditions given in (4.7) and

$$\theta_i \geq 0, i = 1, \ldots, 16, \quad \sum_{i=1}^{20} t m_i I_i(\theta) \leq 1.$$

Here, $m_i = 2$ or 4, see Table 2.

5. Examples

In this section, we give two examples of how the suggested methods work in practice. The first example is based on a discretization of a simulated Boolean model. Boolean models are widely used as simple geometric models for random sets. They are obtained as unions of random particles, attached to uniform points (the germs) in a sampling window. (The particles are independent from one another and from the germs. Also, the model has to be simulated in a window which is larger then the target window to avoid edge effects.) The Boolean model depends on two parameters: The mean number of particles (germs) per unit area and the random particle, also called typical particle. The following simulations have in average 35 particles per unit area. The typical particle

$$K_0 := \alpha\{x = (x_1, x_2) \in \mathbb{R}^2 \,\big|\, \|x\| \leq 1, x_1 \geq 0\}$$

is the right half of the unit disk, randomly scaled with the random variable α, chosen uniformly in $[0.05, 0.15]$. Figure 6 shows a realization of Z and its digitization with respect to the lattice $t\mathbb{Z}^2$, $t = 0.04$.

For the estimation of the mean normal measure, we decreased t to the value 0.01 and estimated the measure as described in Section 4.2, using 2×2 configurations and 3×3 configurations, respectively.

The estimated distributions are conveniently illustrated by the use of the Blaschke body. The Blaschke body $B(Z)$ of Z is a geometrical representation of the mean normal measure. It is (up to translation) the uniquely determined compact convex set whose boundary measure $L(N_Z(\cdot))$ equals $\mathcal{L}$ (see Figure 1 and the definition of N_Z, there). If, for example, Z is isotropic, then $\mathcal{L}$ is up to normalization the uniform distribution

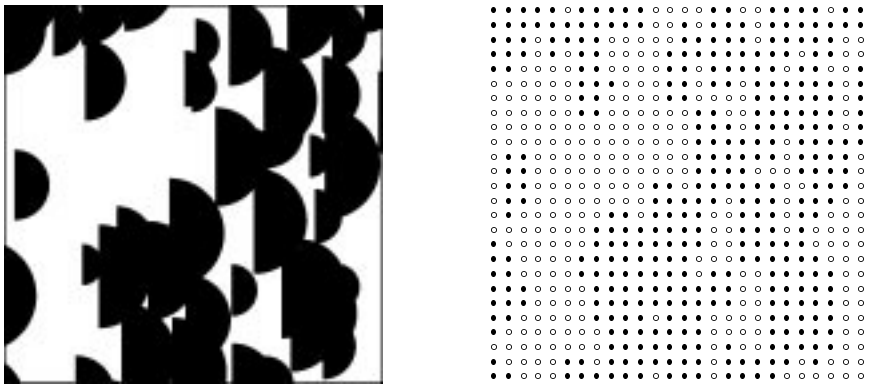

FIGURE 6: Realization of the Boolean model in the unit square and its digitization.

on S^1 and $B(Z)$ is a disc. If Z has a boundary consisting of line segments with finitely many directions, then $\mathcal{L}$ is a measure with finitely many support points and $B(Z)$ is a convex polygon. In the present example, Z is a Boolean model, hence $B(Z)$ is up to translation and scaling equal to the mean typical grain, which is a half-disc. The estimation procedures described yield a (finitely supported) approximation of the mean normal measure. An approximation of the Blaschke body can easily be obtained from these: Order the support points according to increasing angles with respect to the x-axis and draw a polygon as follows: a line segment with the direction of the first support point and length equal to the corresponding mass is drawn (starting e.g. at the origin). At its end-point a line segment with the direction of the second support point and length equal to its mass is appended. Continuation of this procedure for all support points leads to a polygon. The condition (4.7) is crucial now: it guarantees that the polygon will be closed. It is also convex, and its counterclockwise rotation with $90°$ leads to the desired approximation of $B(Z)$.

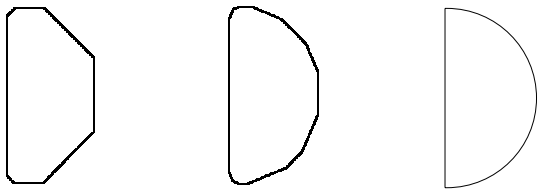

FIGURE 7: Analysis of the Boolean model: The estimates for the Blaschke body for $n = 2$ (left), $n = 3$ (middle) and the exact Blaschke body (right).

The results of the estimation procedure, based on one digitized realization of Z is shown in Figure 7.

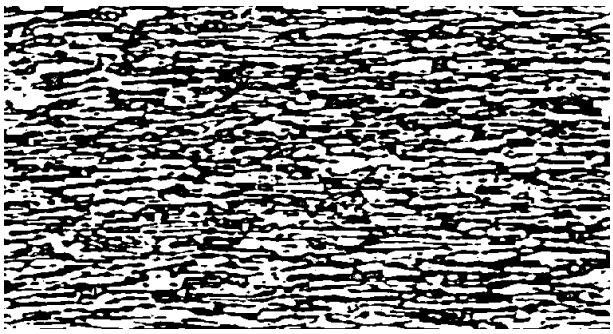

FIGURE 8: Binary image of rolled stainless steel in a longitidial section (courtesy J. Ohser). The white phase is ferrite, the black phase is austenite.

We also analyzed a binary image, showing the microstructure of steel, cf. Figure 8. An earlier analysis can be found in [6], p.137–139, using pairs of pixels only. The estimates of the mean normal measure based on observations of 2×2 and 3×3 configurations, respectively, are shown in Figure 9. Again, the representation in terms of the Blaschke body is used. The estimators are both (almost) centrally symmetric. This indicates that the mean normal measures of black and white phase coincide here.

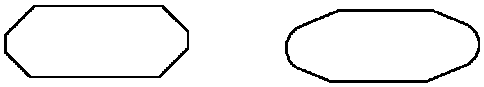

FIGURE 9: The estimators for the Blaschke body of the steel sample in the cases $n = 2$ (left) and $n = 3$.

Finally we want to address the problem of non-sufficient resolution. It is clear that the estimation procedure is unreliable, if the features of Z are very small compared to the scaling t. To quantify this unreliability, we suggest to count the relative number ξ of non-informative configurations, excluding the two configurations of completely black

and completely white $n \times n$ squares. For $n = 2$ there are only two such configurations

$$\begin{bmatrix} \circ & \bullet \\ \bullet & \circ \end{bmatrix}_t \qquad \text{and} \qquad \begin{bmatrix} \bullet & \circ \\ \circ & \bullet \end{bmatrix}_t .$$

The number ξ can be determined together with the numbers of informative configurations. It depends on the scaling t. According to (4.1), ξ is close to 0, if t is sufficiently small. As a rule of thumb, we suggest to accept the resolution if ξ is at most 1%. Otherwise either t or n must be decreased.

6. Some considerations concerning information

According to Table 1, observation of 2×2 configurations gives information about 8 integrals of the type

$$\int_{S^1} h_{a,b}(v) \, \mathrm{d}\mathcal{L}(v), \tag{6.1}$$

where a and b are listed in Table 1. If instead we only compare pairs of points we get information about integrals of the form

$$\frac{1}{2} \int_{S^1} |\langle b \Leftrightarrow w, v \rangle| \, \mathrm{d}\mathcal{L}(v), \tag{6.2}$$

cf. (2.4), where b and w are pairs of different points in the 2×2 lattice square. There are only 4 different values of (6.2) in the 2×2 case. If $\mathcal{L}$ is symmetric the eight values in (6.1) are pairwise equal, and there is no gain of information in considering pairs of subsets instead of pairs of points.

For $n = 3$, the situation is more complex. We have information on 20 integrals of the type (6.1), cf. Table 2, and 8 of the type (6.2). The last 4 integrals of the type (6.1) can be expressed in terms of the 16 previous ones, cf. (4.5), but observing the number of 3×3 configurations of the last 4 types still provides extra statistical information. If $\mathcal{L}$ is symmetric, the 20 values of (6.1) reduce to 10. There is here still a statistical gain in information, considering subsets instead of points.

7. Acknowledgements

We want to express our gratitude to Kim Allan Andersen for his numerical assistance and Joachim Ohser for allowing us to use the steel image. We also want to thank Jane

Vedel for excellent graphical work. This work was supported in part by MaPhySto, funded by a grant from the Danish National Research Foundation.

Appendix A. Proof of Theorem 1

To proof Theorem 1, we first show two lemmas. We will need separation of compact subsets B and W of $\mathbb{R}^2$: B and W are called *separable* if there is a line g such that B and W lie on different sides of g. (More precisely, writing H^+ and H^- for the two *closed* half planes bounded by g, we require $B \subset H^+$ and $W \subset H^-$, or vice versa.) B and $W \subset \mathbb{R}^2$ are called *strictly separable* if there is a line g separating the two sets without hitting them. Two subsets B and W of $\mathbb{L}_n$ are called *n-separable*, if there is an n-lattice line separating B and W and not hitting both of them. n-separation is the digitized notion for strict separation of subsets of $\mathbb{L}_n$:

Lemma 1. *Two subsets B and W of $\mathbb{L}_n$ can be strictly separated if and only if they can be n-separated.*

Proof. Consider $B,\ W \subset \mathbb{L}_n$. Clearly n-separation implies strict separation, as the sets are finite. To show that strict separation implies n-separation, a suitable translation and rotation can be applied to the strictly separating line.

Consider a partition of $\mathbb{L}_n$ consisting of two n-separable subsets B and W. If we are only interested in the set of lines separating B and W, these sets can be replaced by considerably smaller subsets of $\mathbb{L}_n$, see Figure 5. This is made precise in the following lemma, which makes essential use of the regular structure of $\mathbb{L}_n$.

Lemma 2. *Assume B and W are n-separable nonempty, disjoint sets with $B \cup W = \mathbb{L}_n$. Then there are sets $B' \subset B$ and $W' \subset W$ with $|B'| \leq 2,\ |W'| \leq 2$ and such that any line separating B' and W' separates also B and W.*

More precisely, if g is the n-lattice line separating B and W, hitting only B, say, then we can chose B' to consist of the two most distant points in $g \cap B$ and W' to consist of the two (possibly coinciding) most distant points in $\tilde{g} \cap W$ where $\tilde{g}$ is the separating line parallel to g with $\tilde{g} \cap W \neq \emptyset$.

Proof. Let B and W form a partition of $\mathbb{L}_n$ consisting of two nonempty, n-separable sets. As in the formulation of the Lemma, let g be the n-lattice line separating B and W hitting only B and $B' := \{b_1, b_2\}$ be the set of the two most distant points in $B \cap g$. Furthermore, let $\tilde{g}$ be the line parallel to g, separating B and W and hitting W. Let $W' := \{w_1, w_2\}$ be the set of the two most distant points in $W \cap \tilde{g}$. If W' consists of two points, we assume that the lines $h_1 = \text{aff}\{b_1, w_1\}$ ('aff' stands for affine hull) and $h_2 = \text{aff}\{b_2, w_2\}$ have an intersection in the open strip S between g and $\tilde{g}$ (if not, the names of w_1 and w_2 have to be interchanged). Note that the width of S is positive. To show that all lines separating B' and W' also separate B and W, it is enough to show that h_1 and h_2 separate B and W. We concentrate on h_1, the other line can be treated analogously. We show by contradiction that there is no point of W in the open half plane H_{h_1} which is defined by its bounding line h_1 and the assumption $b_2 \in H_{h_1}$. That the other open half plane associated to h_1 contains no points of B can then be treated the same way.

Assume that there is an $a \in W \cap H_{h_1}$ (see Figure 10). As all points of W lie in the closed half plane $H_{\tilde{g}}$ bounded by $\tilde{g}$ and not containing g, we have $a \in H_{h_1} \cap H_{\tilde{g}}$. This wedge can be further restricted by the following consideration: Let b be the point of $(B \cap g) \setminus \{b_1\}$ closest to b_1. We will use later that due to this definition, there are no points in $g \cap \mathbb{L}_n$ between b and b_1 on g. Let $\tilde{h}_1$ be the line parallel to h_1 passing through b, and $H_{\tilde{h}_1}$ the open half plane bounded by $\tilde{h}_1$ containing w_1. We have $a \in H_{\tilde{h}_1}$, for the following reason: If we assume that $a \notin H_{\tilde{h}_1}$, then the point $z := \tilde{h}_1 \cap \tilde{g}$ lies in the convex hull of b, w_1 and a, and as all these points are in $\mathbb{L}_n$, we have $z \in [0, n \Leftrightarrow 1]^2$. But $z \in \mathbb{Z}^2$, as $z = b + (w_1 \Leftrightarrow b_1)$. Thus, $z \in \mathbb{L}_n$, and as $z \in \tilde{g}$ we have $z \in W$, contradicting the property of w_1 being the most distant point from w_2. We conclude that

$$a \in H_{h_1} \cap H_{\tilde{h}_1}, \tag{A.1}$$

i.e. a is contained in a strip parallel to h_1.

Put $v := w_1 \Leftrightarrow b_1 \in \mathbb{Z}^2$ and let $S_g := S \cup g$ the 'one sided closure' of S. As $a \in H_{\tilde{g}}$, there is a unique $m \in \mathbb{N}$ such that a is contained in the shifted strip $S_g + mv$. Hence the shifted point $a' := a \Leftrightarrow mv \in \mathbb{Z}^2$ lies in S_g. As v is the direction of the lines h_1 and

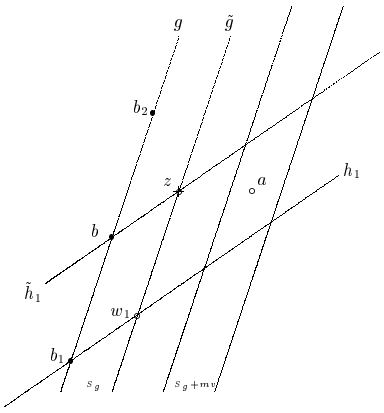

FIGURE 10: Separation of B and W, where only the relevant lattice points are included.

$\tilde{h}_1$, we conclude using (A.1) that

$$a' \in P,$$

where P is the half open parallelogram $S_g \cap H_{h_1} \cap H_{\tilde{h}_1}$. It is clear that a' lies in the convex hull of a, b and b_1 and so, with arguments as before, $a' \in \mathbb{L}_n = B \cup W$. Hence,

$$a' \in P \cap \mathbb{L}_n.$$

But this is impossible, as S does not contain any point of $\mathbb{L}_n$ and g does not contain any point of $\mathbb{L}_n$ between b and b_1. This proves that there are no points in $W \cap H_{h_1}$ and the Lemma is shown.

Proof of Theorem 1

Let (B, W) be an informative configuration. This means that $h_{(B,W)}$ is not identically zero and hence B and W are strictly separable. According to Lemma 1, B and W are $n\Leftrightarrow$separable, so there exist sets $B' \subset B$ and $W' \subset W$, having the properties described in Lemma 2. Using the geometric interpretation of the h function, see e.g. Figure 3, it is clear that $h_{(B,W)} = h_{(B',W')}$. Let $B' = \{b_1, b_2\}$ and $W' = \{w_1, w_2\}$. As at least one of the sets constructed in Lemma 2 consists of two points, we can assume without loss of generality that $b_1 \neq b_2$ and that

$$w_1 \Leftrightarrow w_2 = t(b_1 \Leftrightarrow b_2), \quad \text{for some } t \geq 0. \tag{A.2}$$

We will show that

$$h_{(B',W')}(\Leftrightarrow v) = \min\{\langle w_2 \Leftrightarrow b_1, v\rangle^+, \langle w_1 \Leftrightarrow b_2, v\rangle^+\}, \quad v \in S^1, \tag{A.3}$$

which clearly implies Theorem 1 with $a = w_2 \Leftrightarrow b_1$, $b = w_1 \Leftrightarrow b_2$.

First note that

$$h_{(B',W')}(\Leftrightarrow v) = \left[\min_{w\in W'}\langle w, v\rangle \Leftrightarrow \max_{b\in B'}\langle b, v\rangle\right]^+. \tag{A.4}$$

It is easy to show (A.3) for $t = 0$. For $t > 0$ the condition (A.2) implies that

$$\langle w_1, v\rangle \le \langle w_2, v\rangle \Leftrightarrow \langle b_1, v\rangle \le \langle b_2, v\rangle. \tag{A.5}$$

In order to prove (A.3), suppose that

$$\langle w_1, v\rangle \le \langle w_2, v\rangle. \tag{A.6}$$

Then, because of (A.4) and (A.5), we have

$$h_{(B,W)}(\Leftrightarrow v) = [\langle w_1 \Leftrightarrow b_2, v\rangle]^+ = \min\{\langle w_2 \Leftrightarrow b_1, v\rangle^+, \langle w_1 \Leftrightarrow b_2, v\rangle^+\}.$$

The last equality holds, as (A.5) and (A.6) imply that $\langle w_1 \Leftrightarrow b_2, v\rangle \le \langle w_2 \Leftrightarrow b_1, v\rangle$.

The proof of (A.3) in the case $\langle w_1, v\rangle > \langle w_2, v\rangle$ is analogous.

References

[1] Gardner, R. (1995) *Geometric Tomography*, Cambridge University Press, New York.

[2] Kärkkäinen, S., Jensen, E.B.V., Jeulin, D. (2002) On the orientational analysis of planar fibre systems from digital images, *J. Microsc.* **207**, 69–77.

[3] Kärkkäinen, S., Penttinen, A., Ushakov, N.G., Ushakova, A.P. (2001) Estimation of orientation characteristics of fibrous material, *Adv. Appl. Prob. (SGSA)* **33**, 559–575.

[4] Kiderlen, M., Jensen, E.B.V. (2002) Estimation of the directional measure of planar random sets by digitization, *Submitted.*

[5] Ohser, J., Steinbach, B., Lang, C. (1998) Efficient texture analysis of binary images, *J. Microsc.* **192**, 20–28.

[6] Ohser, J., Mücklich, F. (2000) *Statistical Analysis of Microstructures in Material Science.* Wiley, New York.

[7] Serra, J. (1982) *Image Analysis and Mathematical Morphology*, Vol. 1. Academic Press, London.

[8] Stoyan, D., Kendall, W.S., Mecke, J. (1995) *Stochastic geometry and its applications*, 2nd ed. Wiley, New York.

[9] Weil, W. (1997) Mean bodies associated with random closed sets *Suppl. Rend. Circ. Mat. Palermo* (2) **50**, 387–412.

[10] Weil, W. (1997) The mean normal distribution of stationary random sets and particle processes. In: *Advances in Theory and Applications of Random Sets, Proc. International Symposium, Oct. 9–11, 1996, Fontainebleau, France,* (D. Jeulin, ed.) World Scientific Publ., Singapore, 21–33.